The Joint Power of NOMA and Reconfigurable Intelligent Surfaces in SWIPT Networks

Maria Diamanti*, Eirini Eleni Tsiropoulou†, and Symeon Papavassiliou*
{mdiamanti@netmode.ntua.gr, eirini@unm.edu, papavass@mail.ntua.gr}
* School of Electrical and Computer Engineering, National Technical University of Athens, Athens, Greece
† Dept. of Electrical and Computer Engineering, University of New Mexico, Albuquerque, NM, USA

***Abstract*—Simultaneous Wireless Information and Power Transfer (SWIPT) offers a viable solution for facilitating efficient and sustainable communication networks that serve energy-limited communication devices, as in the forthcoming Internet of Things (IoT) era. Towards exploiting the benefits of SWIPT schemes at their full capacity, achieving both spectral and energy efficiency, Reconfigurable Intelligent Surface (RIS) and Non-Orthogonal Multiple Access (NOMA) technologies allow for effectively treating challenges associated with the low efficiency over long distance and the spectrum scarcity, respectively. In this article, the joint optimization of the RIS elements' phase shifts, the IoT nodes' downlink allocated powers, and their harvested energy, is used as the means to maximize the IoT nodes' sum downlink rate and their weighted uplink data rate. The corresponding optimization problem is formulated as a single-leader multiple-followers Stackelberg game, and solved accordingly, via a distributed and iterative algorithm. The overall proposed optimization framework is evaluated via modeling and simulation, in terms of its spectral efficiency and harvested energy, allowing also to obtain some key insights about the gain provided by the assistance of RIS to a NOMA-operated SWIPT network of IoT nodes.**

***Index Terms*—Simultaneous Wireless Information and Power Transfer, Reconfigurable Intelligent Surfaces, Game Theory.**

I. Introduction

With the advent of Internet of Things (IoT) and the massive Machine-Type Communications (mMTC) scenarios, the number of devices connected in 5G and beyond systems is ever increasing. Towards supporting their energy efficient operation and improved data rates, the application of Non-Orthogonal Multiple Access (NOMA) and Simultaneous Wireless Information and Power Transfer (SWIPT) have emerged as promising technological advances and solutions. The benefits of these approaches have been studied in the current literature, either in a standalone manner or in a combined fashion [1].

At the same time, over the last years the adoption and application of Reconfigurable Intelligent Surface (RIS) facilitates the software-based control over the electromagnetic properties of the wireless environment, thus, combating the unfavorable propagation conditions owing to the wireless channels' fading [2]. This, in turn, allows for the provisioning of superior channel conditions, and consequently, provides reduced transmission power, or equivalently extends the transmission and communications range of the wireless nodes. In this paper, we jointly treat and optimize the downlink and uplink performance of a RIS-aided SWIPT-enabled wireless powered IoT network, operating under NOMA scheme. Our objective is to maximize the IoT nodes' sum downlink data rate and their weighted uplink data rates, by jointly optimizing the RIS elements' phase shifts, the IoT nodes' downlink allocated powers, and their harvested energy due to SWIPT.

This research work was supported by the Hellenic Foundation for Research and Innovation (H.F.R.I.) under the "1st Call for H.F.R.I. Research Projects to support Faculty members and Researchers and the procurement of high-cost research equipment grant" (Project Number: HFRI-FM17-2436). The research of Dr. Tsiropoulou was supported by the NSF CRII-1849739.

A. Related Work

Aiming at supporting multiple users who jointly share the same resource blocks, e.g., subcarrier, time slot, spreading code, NOMA technique has been introduced as part of the 5G and beyond networks. The inherent operational characteristics of NOMA, combined with the Successive Interference Cancellation (SIC) decoding implemented at the receiver, enables the overall network to achieve high throughput, low latency, massive connectivity, improved fairness, and high reliability [3]. In the meanwhile, the SWIPT technology has been proposed to fulfill the communication requirements of energy-constrained devices, while enabling their information exchange with the Base Station (BS). In [4], the authors study a NOMA-enabled SWIPT millimeter-wave network consisting of an aerial BS, which serves as both energy and useful information conveyor. The problem of maximizing the devices' harvested sum-power is examined, while satisfying their personalized minimum data rate constraints. Focusing on the downlink communication, the joint optimization problem of the total transmission data rate and harvested energy is formulated, in [5], as a multi-objective optimization problem with multiple personalized constraints of the devices regarding their minimum rate and harvested energy prerequisites. The joint study of the downlink and uplink in a SWIPT-enabled wireless powered communication network is performed in [6], targeting at optimizing the overall achieved data rate by considering NOMA and Time Division Multiple Access (TDMA) techniques.

Towards further reducing the energy consumption and enhancing the spectral efficiency in 5G and beyond networks, the use of RIS has gained significant attention over the last few years. Typically, a RIS consists of multiple reflecting elements, constructed by engineered metamaterials, whose reflection coefficients can be optimized by a smart controller to provide desirable propagation conditions to the electromagnetic waves, as a software-defined service [2]. Recent works have been devoted to deep reinforcement learning approaches that determine the RIS elements' phase-shift vectors in order to reduce the overhead stemming from the channel estimation and the beam training [7]. The RIS technology has been, also, adopted by [8] within a NOMA-operated cellular network, in order to ensure that the cell-edge users can be served by the BS, via controlling the RIS elements' reflecting coefficients to boost their transmitted beams. In [9], a RIS-assisted NOMA-based wireless network is considered and the authors propose an energy-efficient algorithm that optimizes the tradeoff between the total power consumption minimization and the overall rate maximization. A similar system model is considered in [10], focusing on the uplink communication, where the authors deal with the maximization problem of the sum rate of all users subject to their individual power constraints.

B. Contributions & Outline

In a nutshell, the existing research has exploited the benefits of NOMA, SWIPT, and RIS primarily in a fragmented manner, without revealing their full potential of improving the spectral and energy efficiency in both the downlink and the uplink, which can be realized only by considering the complementarity and integration of the aforementioned technological advances. This paper tackles exactly this issue, while its main contributions are summarized as follows.

1) A system model representing and capturing a RIS-aided NOMA-enabled SWIPT network of IoT nodes paradigm is introduced, examining both the downlink and the uplink communications (Section II).
2) The problem of jointly maximizing the sum rate in the downlink and the weighted data rate of each IoT node in the uplink, while considering the portion of power used to decode the downlink signal, is designed, formulated and treated through a distributed game theoretic approach. The optimization of the RIS elements' phase shifts, the IoT nodes' downlink allocated powers, and their harvested energy, is used as the means to realize the above objective, and is obtained via a single-leader multiple-followers Stackelberg game (Section III-A).
3) The RIS elements' phase shifts and the IoT nodes' downlink allocated powers are formulated as two sequential optimization problems solved at the hybrid access point, i.e., the leader (Section III-B). The IoT nodes' energy harvesting optimization is solved in a distributed manner by each IoT node, i.e., the follower (Section III-C).
4) Indicative numerical results are presented that demonstrate the benefits in terms of spectral efficiency and harvested energy, obtained by jointly exploiting the capabilities of the NOMA, SWIPT, and RIS technologies (Section IV).

II. System Model

A RIS-aided and NOMA-operated SWIPT network is considered, as illustrated in Fig. 1, consisting of a Hybrid Access Point (HAP), which transmits signals to $|N|$ IoT nodes, with

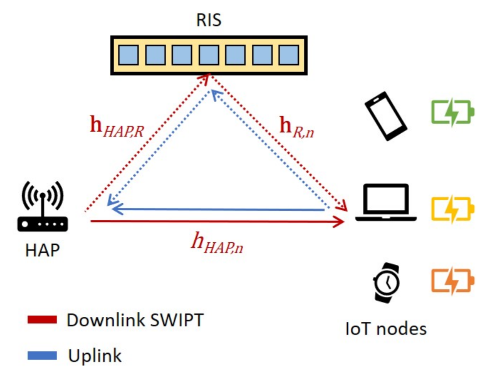

Fig. 1: Overview of the RIS-aided and NOMA-enabled SWIPT network of IoT nodes.

$N = \{1, \dots, n, \dots, |N|\}$ denoting their set, and serves as both energy and useful information conveyor. Both the HAP and the IoT nodes bear single-antenna receivers and transmitters, while perfect Channel State Information (CSI) knowledge is assumed in the system. The overall network's operation is divided in time slots, considering a single time slot's t duration to be 1 time unit for simplicity in the notation. Each time slot t comprises of the downlink and uplink transmission phases of durations τ and $1-\tau$ time units, accordingly.

The downlink transmission power allocated to each IoT node n by the HAP is denoted as P_n^d [W] and it holds that $\sum_{n=1}^{|N|} P_n^d \leq P_{HAP}^{max}$, where P_{HAP}^{max} [W] is the HAP's downlink power budget. During the downlink phase, each IoT node exploits the $\lambda_n \sum_{n=1}^{|N|} P_n^d$ part of the HAP's downlink transmission power to decode the received information message, and the rest $(1-\lambda_n) \sum_{n=1}^{|N|} P_n^d$ amount of power is used to harvest energy and charge its device. The factor $\lambda_n \in [0,1], \forall n \in N$ denotes the power splitting ratio between the power used for decoding and energy harvesting. The IoT node's n harvested energy due to SWIPT is $E_n = \eta G_n \tau (1-\lambda_n) \sum_{n=1}^{|N|} P_n^d$ [J], where $\eta \in (0,1)$ constitutes the IoT node's energy harvesting efficiency factor and G_n is the channel power gain between the HAP and the IoT node n.

By implementing the RIS technology, the total channel power gain G_n between the HAP and the IoT node n, during the downlink phase, is determined as follows. Consider a RIS consisting of $|M|$ reflecting elements in the form of a uniform linear array, with $M = \{1, \dots, m, \dots, |M|\}$ denoting their set, placed at a height of z_R [m] above the ground. The diagonal phase-shift matrix is $\boldsymbol{\omega} = diag\{e^{j\omega_1}, \dots, e^{j\omega_{|M|}}\}$, where $\omega_m \in [0, 2\pi)$, $\forall m \in M$, while the first RIS element is used as a reference point for the performance of the subsequent calculations. The direct link between the HAP and the IoT node n exhibits Rayleigh fading and its channel gain is modeled as $h_{HAP,n} = \sqrt{\rho d_{HAP,n}^{-k}} \tilde{h} \in \mathbb{C}$, where ρ is the path loss at the reference distance 1 m, $d_{HAP,n}$ [m] is the euclidean distance between the HAP and the node n, k is the path loss exponent, and $\tilde{h} \backsim \mathcal{CN}(0,1)$ is the random scattering component captured by a zero-mean and unit-variance complex Gaussian random variable. Assuming that the RIS is in close proximity to the HAP and a Line-of-Sight (LoS) path exists between them, their in-between channel gain is $\mathbf{h}_{HAP,R} = \sqrt{\rho d_{HAP,R}^{-2}}[1, e^{-j\frac{2\pi}{\lambda}d\phi_{HAP,R}}, \dots, e^{-j\frac{2\pi}{\lambda}(|M|-1)d\phi_{HAP,R}}]^T \in \mathbb{C}^{|M|\times 1}$, where λ [m] is the carrier wavelength, d [m] is the antenna separation, $d_{HAP,R}$ [m] is the euclidean distance between the HAP and the reference point of RIS and $\phi_{HAP,R}$ is the cosine of the angle of arrival of the signal from the HAP to the RIS. Due to the RIS and its strong reflection signal, the channel between the RIS and the IoT node is exposed to Rician fading and its channel gain is modeled as $\mathbf{h}_{R,n} = \sqrt{\rho d_{R,n}^{-a}}(\sqrt{\frac{\beta}{1+\beta}}\mathbf{h}_{R,n}^{LoS} + \sqrt{\frac{1}{1+\beta}}\mathbf{h}_{R,n}^{NLoS}) \in \mathbb{C}^{|M|\times 1}$, where a is the path loss exponent in the examined link, β is the Rician factor, $\mathbf{h}_{R,n}^{LoS} = [1, e^{-j\frac{2\pi}{\lambda}d\phi_{R,n}}, \dots, e^{-j\frac{2\pi}{\lambda}(|M|-1)d\phi_{R,n}}]^T$ is the LoS component, $\mathbf{h}_{R,n}^{NLoS} \backsim \mathcal{CN}(0,1)$ is the Non-LoS (NLoS) component and $\phi_{R,n}$ is the cosine of the angle of departure of the signal from the RIS to the IoT node. For simplicity, we write $\mathbf{h}_{R,n}$, as $\mathbf{h}_{R,n} = [|h_{R,n,1}|e^{j\Phi_1}, \dots, |h_{R,n,m}|e^{j\Phi_m}, \dots, |h_{R,n,|M|}|e^{j\Phi_{|M|}}]^T$. The total channel power gain between the HAP and IoT node n in the downlink is given by $G_n = |h_{HAP,n} + \mathbf{h}_{R,n}^H \boldsymbol{\omega} \mathbf{h}_{HAP,R}|^2$. Capitalizing on the property of channel reciprocity that holds for Time Division Duplex (TDD) systems and considering that RIS metamaterials conform to the channel reciprocity theorem, as stated in [11], we assume that the total uplink channel power gain is, also, equal to G_n.

Each IoT node n performs SIC to decode its downlink transmitted signal, considering without loss of generality that it holds: $\lambda_1 G_1 \leq \dots \leq \lambda_n G_n \leq \dots \lambda_{|N|} G_{|N|}$. Thus, each IoT node's n achievable downlink data rate is:

$$R_n^d = \tau \log_2(1 + \frac{G_n \lambda_n P_n^d}{G_n \lambda_n \sum_{i=n+1}^{|N|} P_i^d + I_0})[bps/Hz], \quad (1)$$

where I_0 is the power of zero-mean Additive White Gaussian Noise (AWGN).

Focusing on the uplink communication, each IoT node n utilizes exclusively the harvested energy E_n to transmit its data to the HAP and its uplink transmission power is $P_n^u = \frac{E_n}{1-\tau}$. Thus, each IoT node's n uplink data rate is given as follows:

$$R_n^u = (1-\tau)\log_2(1 + \frac{G_n P_n^u}{\sum_{i=1}^{n-1} G_i P_i^u + I_0})[bps/Hz]. \quad (2)$$

III. Joint Phase Shift, Power, and Energy Harvesting Optimization

A. Problem Description and Design

The key objective of our work is to jointly maximize the sum rate in the downlink and the weighted data rate of each IoT node in the uplink, while accounting for the portion of power used to properly decode the downlink signal. Within our setting and considered model, this objective is realized via the joint RIS elements' phase shifts, the IoT nodes' downlink allocated powers, and their harvested energy optimization. The joint optimization problem is formulated as a distributed single-leader multiple-followers Stackelberg game. In particular, the HAP acts as the leader determining the effective RIS elements' phase shifts and the downlink allocated powers to the IoT nodes via two sequential optimization problems. The results are fed back to the RIS controller and the IoT nodes via dedicated control links. Then, the IoT nodes act as followers determining in a distributed and autonomous manner their optimal power splitting ratios (i.e., λ_n), thus, deriving the optimal amount of harvested energy. The goal of the HAP is to maximize the sum rate in the downlink and the goal of the IoT nodes is to maximize their personal weighted uplink data rate, while considering the portion of power used to decode their received downlink signal. The Stackelberg game is played iteratively during a time slot in order to converge to the Stackelberg equilibrium, as shown in Fig. 2.

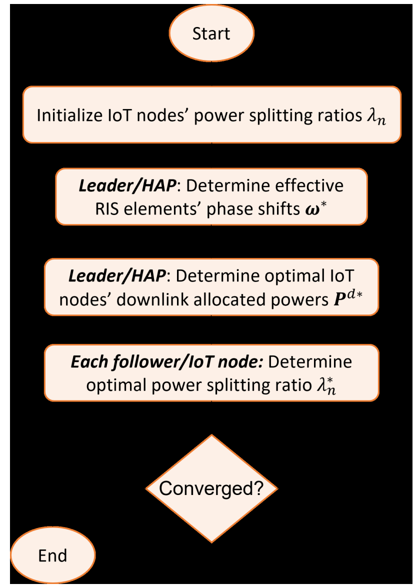

Fig. 2: Optimization process and control flow.

B. Phase Shift and Downlink Power Optimization

The HAP determines the effective RIS elements' phase shifts $\boldsymbol{\omega}^* = [\omega_1^*, \dots, \omega_m^*, \dots, \omega_{|M|}^*]$ and the optimal downlink allocated powers $\mathbf{P}^{d*} = [P_1^{d*}, \dots, P_n^{d*}, \dots, P_{|N|}^{d*}]$ given the IoT nodes' power splitting ratio vector $\boldsymbol{\lambda} = [\lambda_1, \dots, \lambda_n, \dots, \lambda_{|N|}]$, towards maximizing the sum downlink rate. The optimization problem is formulated as follows:

$$\max_{\boldsymbol{\omega}, \mathbf{P}^d} \sum_{n=1}^{|N|} R_n^d(\boldsymbol{\omega}, \mathbf{P}^d, \boldsymbol{\lambda}) \quad (3a)$$

$$\text{s.t.} \quad \sum_{n=1}^{|N|} P_n^d \leq P_{HAP}^{max} \quad (3b)$$

$$0 \leq \omega_m < 2\pi, \forall m \in M \quad (3c)$$

$$G_n \lambda_n P_{n-1}^d - G_n \lambda_n \sum_{i=n}^{|N|} P_i^d \geq P_{tol}, n = 2, \dots, |N| \quad (3d)$$

$$P_n^u \leq P_n^{max}, \forall n \in N \quad (3e)$$

$$R_n^d \geq R_{min}^d, \forall n \in N, \quad (3f)$$

where Eq. (3b) ensures the HAP's downlink power budget, Eq. (3c) indicates the feasible range of RIS elements' phase shifts, Eq. (3d) ensures the successful SIC decoding at the IoT nodes' receivers based on their sensitivity P_{tol}, Eq. (3e) ensures that the nodes' harvested energy is such that their maximum power budget is not exceeded and Eq. (3f) captures the minimum downlink data rate constraint of each IoT node.

To treat the two-variable optimization problem in a tractable manner, two sequential sub-problems are designed and solved. First, the RIS elements' effective phase shifts are determined so as to maximize the downlink signal strength and hence, the downlink achieved data rate of each IoT node. Assuming a single-node case, the IoT node's signal strength is maximized when the HAP-to-node and RIS-to-node signals are coherently added, leading to the following phase shifts' adaptation:

$$\omega_m^* = \angle\tilde{h} + \Phi_m + \frac{2\pi}{\lambda}d(m-1)\phi_{HAP,R}, \forall m \in M. \quad (4)$$

In the multi-node case considered in this paper, Eq. (4) gives different phase-shift adaptations for different nodes. Thus, for practical purposes, the linear combination approach proposed in [12] is adopted to conclude to a single phase-shift vector $\boldsymbol{\omega}^*$. Specifically, a set of appropriate weights is found for each node, such that the linear combination of the phase shifts derived from Eq. (4) for each node separately, yields the maximum overall nodes' signal strength.

Given the effective RIS elements' phase shifts, the optimization problem in Eq. (3a)-(3f) can be written as follows:

$$\max_{\mathbf{P}^d} \sum_{n=1}^{|N|} R_n^d(\boldsymbol{\omega}, \mathbf{P}^d, \boldsymbol{\lambda}) \quad (5a)$$

$$\text{s.t.} \quad \sum_{n=1}^{|N|} P_n^d \leq P_{HAP}^{max} \quad (5b)$$

$$G_n\lambda_n P_{n-1}^d - G_n\lambda_n \sum_{i=n}^{|N|} P_i^d \geq P_{tol}, n = 2, \ldots, |N| \quad (5c)$$

$$P_n^u \leq P_n^{max}, \forall n \in N \quad (5d)$$

$$R_n^d \geq R_{min}^d, \forall n \in N. \quad (5e)$$

The optimization problem is concave and can be solved using the Karush–Kuhn–Tucker (KKT) conditions to derive the optimal downlink allocated powers to the IoT nodes $\mathbf{P}^{d*}$.

C. Energy Harvesting Optimization

Given the RIS elements' phase shifts and the downlink allocated powers as determined above, each IoT node aims at maximizing its weighted data rate, while accounting for the portion of power used to decode its downlink signal. The optimization problem to be solved by each IoT node is:

$$\max_{\lambda_n} \lambda_n^\xi R_n^u(\boldsymbol{\omega}, \mathbf{P}^d, \boldsymbol{\lambda}) \quad (6a)$$

$$\text{s.t.} \quad 0 \leq \lambda_n \leq 1, \forall n \in N \quad (6b)$$

$$P_n^u \leq P_n^{max}, \forall n \in N \quad (6c)$$

$$G_n P_n^u - \sum_{i=1}^{n-1} G_i P_i^u \geq P_{tol}, n = 2, \ldots, |N| \quad (6d)$$

$$R_n^u \geq R_{min}^u, \forall n \in N. \quad (6e)$$

The term λ_n^ξ in Eq. (6a) indicates the IoT node's evaluation of its power splitting ratio λ_n among the downlink signal decoding and the harvested energy, where the latter one is used for the uplink data transmission to the HAP. By appropriately tuning the parameter ξ, the IoT node can achieve different power splitting ratio regions, and thus, it can satisfy different Quality of Service (QoS) requirements. Also, Eq. (6b) and Eq. (6c) indicate the feasible range of values of the power splitting ratio λ_n and the uplink transmission power P_n^u, Eq. (6d) guarantees the successful SIC at the HAP's receiver and Eq. (6e) reassures the minimum QoS prerequisites of the IoT node in terms of achieved uplink data rate.

The above optimization problem can be treated as a non-cooperative game among the IoT nodes, where each node aims at maximizing its payoff function, as shown in Eq. (6a). Each IoT node performs its distributed decision-making and determines its optimal power splitting ratio λ_n^*, by receiving the information of its sensed interference, as presented in Eq. (2), via broadcasting by the HAP, until a Nash equilibrium is reached. The IoT nodes conclude to a Nash equilibrium, which is a stable operation point of the overall system [13]. The two optimization problems in Eq. (5a)-(5e) and Eq. (6a)-(6e), are solved iteratively and sequentially, and the output of the one acts as input to the other, following the relationship of the leader and the followers. This iterative procedure concludes to the Stackelberg equilibrium.

IV. Evaluation & Results

To evaluate the overall performance of our proposed framework in terms of spectral efficiency and harvested energy, and in particular to obtain some insight about the gain provided by the assistance of RIS in a NOMA-enabled SWIPT network, we consider the following network topology. A HAP is located at the origin of a typical 3D coordinate system and the reference point of a RIS consisting of $|M|$ reflecting elements is placed 1m away from the HAP at the x axis and at a height of $z_R = 1.5$m above the ground. $|N| = 3$ IoT nodes are placed with increasing distances from the HAP along the $y = x$ line, forming a NOMA cluster. The IoT nodes' distances along the $y = x$ line are d_1 [m], $d_1 + 2$ [m] and $d_1 + 4$ [m], respectively, where d_1 denotes the distance of the first node. In the following, different scenarios regarding the IoT nodes' distances from the HAP and the RIS are analyzed and indicated by the first IoT node's distance d_1. The remaining parameters are set as follows: $\tau = 0.7$, $P_{HAP}^{max} = 20$W, $P_n^{max} = 0.2$W, $\eta = 0.6$, $\rho = 0.01$, $k = 3.5$, $d = \frac{\lambda}{2}$, $a = 2.8$, $\beta = 2$, $I_0 = -114$dBm, $P_{tol} = -121$dBm, $R_{min}^d = R_{min}^u = 1$bps/Hz and $\xi = 0.5$. The results have been averaged over 100 different channel model realizations.

In Fig. 3a, the IoT nodes' sum downlink (DL) and sum uplink (UL) data rate is presented in the y axis (bps/Hz) with respect to different IoT nodes' distances scenarios in the x axis, after performing the joint optimization described in Fig. 2. The results have been extracted considering a number of $|M| = 50$ RIS elements, while the cases of existence and non-existence of the RIS within the network topology are

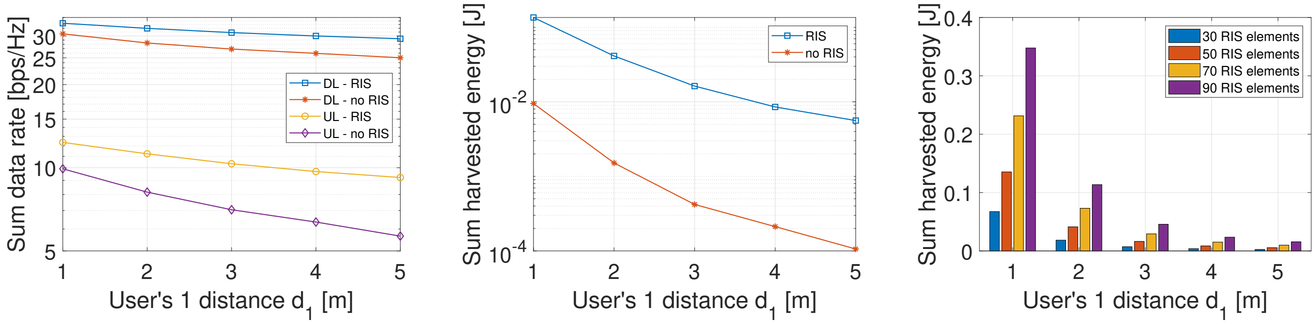

(a) (b) (c)

Fig. 3: Spectral efficiency and harvested energy evaluation of the RIS-aided and NOMA-enabled SWIPT network.

indicated as "RIS" and "no RIS", respectively. It is confirmed that the use of RIS results in significantly higher sum data rates in both communication directions, by enhancing the IoT nodes' channel gains via the strong reflected LoS link. The sum data rates, also, remain relatively sustained as the IoT nodes' distances increase, compared to the situation where no RIS exists and the sum data rates degrade faster.

The increased channel gains allow for the IoT nodes' increased energy harvesting during the downlink wireless power transfer phase. This behavior is corroborated by Fig. 3b, in which the sum harvested energy of the IoT nodes is depicted in the y axis, as a function of the different distances scenarios in the x axis, considering $|M| = 50$ RIS elements. The results show that the use of RIS can provide almost two orders of magnitude higher sum harvested energy in the most demanding case, where the IoT nodes' distances from the HAP are 5m, 7m and 9m respectively.

In order to investigate the effect of RIS size on the SWIPT network's performance, Fig. 3c presents the sum IoT nodes' harvested energy with respect to various distances scenarios, under a different number of RIS elements analysis, i.e., for $|M| = \{30, 50, 70, 90\}$. In the first two distance scenarios, where the IoT nodes are near the HAP and the RIS, they reap the benefits of the increased number of RIS elements and achieve a notably high sum harvested energy. However, as the IoT nodes' distances become higher, the effect of the increased number of RIS elements diminishes.

V. Conclusion and Future Work

In this paper, a wireless powered communication IoT paradigm is introduced, capitalizing on the joint exploitation of the key benefits of NOMA, SWIPT, and RIS technologies. Towards achieving spectral and energy efficiency both in the downlink and uplink communication simultaneously, the joint optimization of the RIS elements' phase shifts, the IoT nodes' downlink allocated powers, and their energy harvesting, is modeled and formulated as a Stackelberg game among the hybrid access point and the IoT nodes. Indicative numerical results highlight the benefits of the joint exploitation of the RIS technology within the context of NOMA-enabled SWIPT IoT networks. Part of our current and future work contains the extension of the presented model by jointly considering the optimal deployment of the RIS within the examined topology, while accounting for user mobility as well.

References

[1] T. D. Ponnimbaduge Perera, D. N. K. Jayakody, S. K. Sharma, S. Chatzinotas, and J. Li, "Simultaneous wireless information and power transfer (swipt): Recent advances and future challenges," *IEEE Communications Surveys Tutorials*, vol. 20, no. 1, pp. 264–302, 2018.

[2] X. Yuan, Y. J. Angela Zhang, Y. Shi, W. Yan, and H. Liu, "Reconfigurable-intelligent-surface empowered wireless communications: Challenges and opportunities," *IEEE Wirel. Comm.*, pp. 1–8, 2021.

[3] Z. Ding, X. Lei, G. K. Karagiannidis, R. Schober, J. Yuan, and V. K. Bhargava, "A survey on non-orthogonal multiple access for 5g networks: Research challenges and future trends," *IEEE Journal on Selected Areas in Communications*, vol. 35, no. 10, pp. 2181–2195, 2017.

[4] J. Cui, M. B. Khan, Y. Deng, Z. Ding, and A. Nallanathan, "Unsupervised learning approaches for user clustering in noma enabled aerial swipt networks," in *IEEE SPAWC*, 2019, pp. 1–5.

[5] J. Tang, Y. Yu, M. Liu, D. K. C. So, X. Zhang, Z. Li, and K. Wong, "Joint power allocation and splitting control for swipt-enabled noma systems," *IEEE Trans. on Wir. Comm.*, vol. 19, no. 1, pp. 120–133, 2020.

[6] P. D. Diamantoulakis, K. N. Pappi, and G. K. Karagiannidis, "Jointly optimal downlink/uplink design for wireless powered networks," in *24th International Conference on Telecommunications (ICT)*, 2017, pp. 1–6.

[7] A. Taha, Y. Zhang, F. B. Mismar, and A. Alkhateeb, "Deep reinforcement learning for intelligent reflecting surfaces: Towards standalone operation," in *IEEE SPAWC*, 2020, pp. 1–5.

[8] Z. Ding and H. Vincent Poor, "A simple design of irs-noma transmission," *IEEE Comm. Letters*, vol. 24, no. 5, pp. 1119–1123, 2020.

[9] F. Fang, Y. Xu, Q. V. Pham, and Z. Ding, "Energy-efficient design of irs-noma networks," *IEEE Transactions on Vehicular Technology*, vol. 69, no. 11, pp. 14 088–14 092, 2020.

[10] M. Zeng, X. Li, G. Li, W. Hao, and O. A. Dobre, "Sum rate maximization for irs-assisted uplink noma," *IEEE Communications Letters*, vol. 25, no. 1, pp. 234–238, 2021.

[11] W. Tang, X. Chen, M. Z. Chen, J. Y. Dai, Y. Han, S. Jin, Q. Cheng, G. Y. Li, and T. J. Cui, "On channel reciprocity in reconfigurable intelligent surface assisted wireless network," *arXiv preprint:2103.03753*, 2021.

[12] B. Zheng, Q. Wu, and R. Zhang, "Intelligent reflecting surface-assisted multiple access with user pairing: Noma or oma?" *IEEE Communications Letters*, vol. 24, no. 4, pp. 753–757, 2020.

[13] E. E. Tsiropoulou, G. K. Katsinis, and S. Papavassiliou, "Distributed uplink power control in multiservice wireless networks via a game theoretic approach with convex pricing," *IEEE Transactions on Parallel and Distributed Systems*, vol. 23, no. 1, pp. 61–68, 2011.